MASSACHUSETTS INSTITUTE OF TECHNOLOGY

WAVE COUPLING EFFECTS IN THE NONLINEAR EVOLUTION OF THE BEAM-PLASMA INSTABILITY

by

A.L. Throop and R.R. Parker

PFC/JA-79-7
April 1978

PLASMA FUSION CENTER

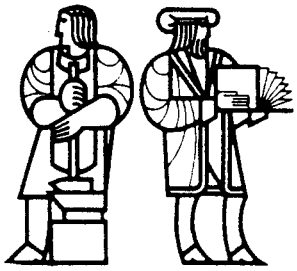

ASSOCIATED WITH

DEPARTMENT OF ELECTRICAL ENGINEERING
AND COMPUTER SCIENCE
DEPARTMENT OF NUCLEAR ENGINEERING
DEPARTMENT OF PHYSICS
FRANCIS BITTER NATIONAL MAGNET LABORATORY
RESEARCH LABORATORY OF ELECTRONICS

Wave coupling effects in the nonlinear evolution of the beam-plasma instability

A. L. Throop[a] and R. R. Parker

Research Laboratory of Electronics and Department of Electrical Engineering and Computer Science, Massachusetts Institute of Technology, Cambridge, Massachusetts 02139
(Received 7 April 1978)

A formalism is presented which has been used to study the nonlinear evolution of the reactive beam-plasma instability in the presence of wave coupling. Special consideration is given to describing the energy of the unstable mode in deriving the coupled-mode equations, and this results in a four-wave model for the interaction. The results show that pump depletion can stabilize the linear instability, and also predict transitional behavior in saturation mechanisms which is observed experimentally.

I. INTRODUCTION

The interaction of electron beams with a background plasma has been studied intensively for several years.[1] Recent work has focused largely on describing the nonlinear evolution of the interaction,[2] since it presents one of the simplest nonlinear systems available while offering a variety of physical phenomena, depending upon specific conditions of the experiment or assumed model.

Several beam-plasma experiments have reported parametric decay processes involving the unstable beam-plasma mode as one of the interacting waves.[3-6] It has been observed that such wave-wave couplings can dominate over other nonlinear mechanisms to stabilize the linear growth of the beam-plasma wave by pump depletion.[3,4] In addition, beam trapping and parametric decay have been found to act as competing saturation mechanisms, each dominating over a different range of experimental conditions.[4,5] In this paper we discuss a model for the early nonlinear evolution of the reactive beam-plasma instability which views the interaction as a four-wave resonant coupling. The model presents an interesting extension to the well-understood three-wave problem and predicts stabilizing effects on the linear beam-plasma instability due to parametric decay, as well as transitional behavior with competing saturation mechanisms.

This work has focused largely on the results of an experiment which has been described previously.[3] The linear dispersion relation for this experiment, describing radial eigenmodes propagating in the direction of the beam flow $\mathbf{v}_b$, is given by

$$\mathfrak{D}(\omega, k_z) = 1 + \frac{k_\perp^2}{k_z^2} - \sum_s \frac{\omega_{ps}^2}{\omega_D^2} \frac{1 + (k_\perp^2/k_z^2)(1/f_s)}{1 - (\alpha_{ts}^2/\omega_D^2)(k_z^2 + k_\perp^2/f_s)} = 0 \tag{1}$$

where $k_\perp$ is the radial eigenmode of the system which is determined by the beam radius, $f_s \equiv 1 - \Omega_s^2/\omega_D^2$, $\Omega_s = q_s B_0/m_s$, $\alpha_{ts}^2 \equiv \gamma v_{ts}^2 = \gamma k T_s/m_s$, γ is the ratio of specific heat, and $\omega_D = \omega - \mathbf{k}_z \cdot \mathbf{v}_b$. The sum is over all plasma species. This dispersion relation is shown in Fig. 1 for conditions of the experiment. A weak electron beam (1 mA, 1000 V), which independently supports fast and slow space-charge waves, is injected coaxially into a magnetized background plasma to cause reactive growth of the beam modes by the linear beam-plasma instability. The reactive nature of the linear coupling causes the two beam waves to form conjugate beam-plasma modes as shown, with the same real frequency and wavenumber but with equal growth and decay rates. These two modes, along with the two nonlinear decay products, form a system of four coupled waves. The beam is current modulated to obtain a well-defined, convectively unstable beam-plasma wave (labeled B in the figure) which is experimentally observed to grow until its amplitude becomes sufficiently large so that it is able to resonantly decay into a backward-propagating Trivelpiece–Gould mode (labeled T) and a forward-traveling ion-acoustic mode (labeled A) of the plasma column. It is observed that saturation in spatial growth of the beam-plasma wave coincides with the onset of parametric decay and that a significant fraction of the beam-plasma energy can be resonantly lost to the T mode. Wave coupling effects occur for both modulated and free-running beams and are strongest over well-defined ranges of beam frequency, beam energy, and background plasma density. Within these ranges there is no evidence of spectra due to other saturation mechanisms. Figure 2 shows the well-defined spectra of the pump and decay modes obtained for the modulated case.

In studying the parametric interaction, mode energies must be carefully considered since the interaction in-

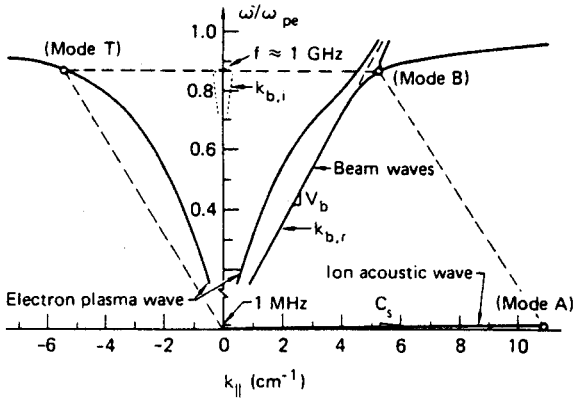

FIG. 1. Linear dispersion relation for the reactive beam-plasma instability.

[a]Present address: Lawrence Livermore Laboratory, Livermore, Calif. 94550.

 0031-9171/79/030491-16$00.90

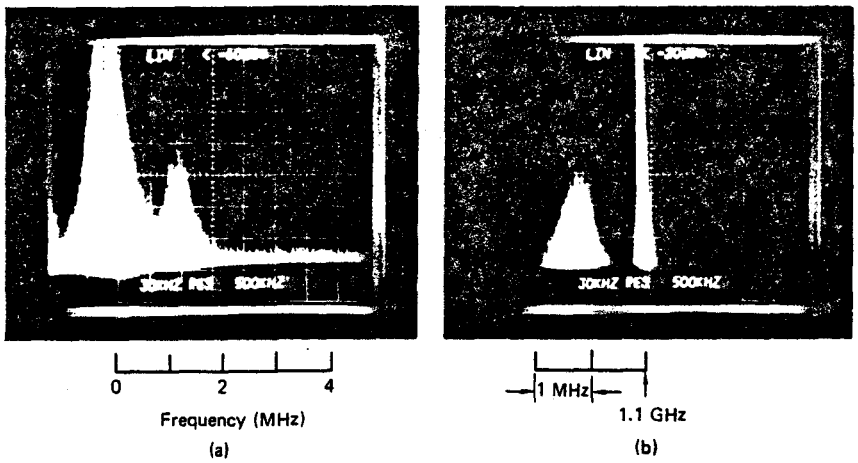

FIG. 2. Spectrum of the beam-driven parameter decay instability: (a) low-frequency fluctuations and ion-acoustic spectrum; (b) corresponding high-frequency spectrum showing narrow beam-plasma wave and Trivelpiece–Gould spectrum.

volves an energy loss process from a high-frequency pump mode which has negative energy in the uncoupled state. Such a situation is usually explosively unstable, and would then serve only to enhance the growth of the beam-plasma mode. In Sec. II a generalized energy conservation theorem is used to derive a resonant wave-coupling model for the parametric decay instability as driven by the reactively unstable beam-plasma mode. The formalism permits one to properly treat the small-signal energy of the unstable mode, to discuss its significance in the context of the full nonlinear theory, and requires that the interaction be viewed as a four-wave, rather than as a three-wave, coupling.

Section III discusses the nonlinear evolution of the coupled-mode system for the special cases of the space-independent and time-independent set of equations. The results of an analytical and numerical analysis for each case are summarized, and conditions necessary for the nonlinear stability of the system are established. The dependence of saturation amplitude and turning point distance on initial mode amplitudes, linear growth rates, and coupling coefficient are studied. Similarities to the three-wave case and its relevance to the time-asymptotic state of this system are discussed.

Section IV discusses the predictions of this theory over parameter ranges relevant to this wave-coupling experiment and to several others where beam trapping has been observed as the dominant saturation mechanism. The results suggest that stabilization of the unstable beam-plasma wave by parametric decay is possible over the parameter range of this experiment, and that wave coupling should be important early in the development of the beam-plasma interaction before beam trapping can occur. Scaling laws obtained from the numerical integration of the coupled mode equations are used to identify sensitive experimental parameters which determine the saturated amplitude of the beam-plasma interaction. The results predict that parametric decay effects should dominate for those cases involving strong linear growth rates or frequencies near the maximum growth rate, while beam trapping effects should dominate for weaker beam-plasma instabilities or at frequencies removed from the maximum growth rate region. These predictions are compared with experimental observations.

II. DERIVATION OF THE INTERACTION MODEL

In this section we describe the formalism used to derive coupled-mode equations for the reactive beam-plasma instability and subsequent wave-wave coupling. The approach used for this model is analogous to that used for the three-wave case. The energy transferred between modes is assumed to modify the linear wave amplitudes through a slowly-varying component $a(\bar{r},t)$, which is introduced to describe the first-order solution on a longer time scale than the linear equations would otherwise permit. The behavior of $a(\bar{r},t)$ is described (for the three wave case) by a coupled mode equation of the form

$$(d/dt)a_A = Ka_T a_B , \tag{2}$$

where the capitalized subscripts denote the coupled waves, K is the coupling coefficient, $d/dt \equiv \partial/\partial t + \mathbf{v}_{gM}\cdot\nabla$ occurs on a time scale slow compared with ω^{-1}, and $\mathbf{v}_{gM} \equiv \partial\omega/\partial \mathbf{k}|_M$ is the group velocity of (any) mode M. Equations similar to (2) are written for each mode, and the resulting set of nonlinear equations is solved to obtain the nonlinear evolution of the system. The coupled-mode equation is obtained from a conservation equation of the form

$$\frac{\partial}{\partial t} w_M + \nabla\cdot \mathbf{s}_M + p_{d,M} = p_{e,M} \tag{3}$$

which is derived for our model using a generalized energy theorem. Here, w_M and $\mathbf{s}_M$ are the small-signal energy and power flow, $p_{d,M}$ represents the power dissipation and $p_{e,M}$ represents an external source term driving mode M. The source term arises from the nonlinear coupling, and gives rise to the spatial and temporal changes in mode energy. Initially, we neglect the linear dissipative effects represented by p_d. However, the linear beam-plasma interaction is a reactive type of instability and the formalism forces one to account explicitly for the finite growth and decay rates of the beam-plasma waves. In order to obtain a proper time-scale matching of the nonlinear equations on both sides of (3), the parametric interaction is described as a four-wave coupling involving the two plasma modes A and T, and the growing and decaying beam-plasma waves (which are denoted G and D, respectively). The formalism leads to a coupling coefficient that is complex, instead of the usual form which is either purely real or

imaginary.[7] It is found that K contains resonant terms as a result of the presence of the beam-plasma modes, and that the wave coupling can become very strong near the maximum growth rate of the linear instability. The formalism indicates that the small-signal energy of either beam-plasma mode taken independently, w_G or w_D, is identically zero. Instead, a complex quantity denoted $\tilde{w}_B$, formed by a combination of both beam-plasma modes, is used to derive coupled-mode equations for modes G and D. We find that $\tilde{w}_B$ can still be written in the usual form for mode energy as $\epsilon_0 E_B^2 \omega(\partial/\partial\omega)\mathfrak{D}$, where $\mathfrak{D}(\omega, k)$ is the dispersion relation, if this quantity is now evaluated at the complex frequency $\tilde{\omega}_B = \omega_B + j\gamma$ (note the twiddle convention for complex quantities). Using this form for mode energy, one can obtain four coupled-mode equations describing the space-time behavior of the interacting waves.

A. Derivation of the generalized conservation theorem

The modes of interest are all lightly damped and $k\lambda_{De} \ll 1$, so that kinetic effects may be neglected. We therefore use a three-fluid model for the system to derive an energy theorem similar to Eq. (3). We combine the force and continuity equations for each of the three plasma species, together with Poisson's equation, to obtain a form for the conservation equation that is commensurate with the form of a coupled-mode equation. In the following, zero- and first-order plasma variables (density n, velocity v) for the plasma electrons, ions, and electron beam are written, respectively, as:

$$n = n_0 + n_e, \quad v = v_e, \quad \ldots \text{electrons},$$
$$n = n_0 + n_i, \quad v = v_i, \quad \ldots \text{ions},$$
$$n = n_b + n_\beta, \quad v = v_b + v_\beta, \quad \ldots \text{beam}.$$

The seven fluid equations in the resulting set are written twice, once as an uncoupled set of linearized equations, and again as a coupled set of nonlinear equations whose solutions have a slow time variation as a result of the nonlinear driving terms. The two sets of equations then become

Linear set

$$\frac{\partial n_e}{\partial t} + \nabla\cdot(n_0 \mathbf{v}_e) = 0, \tag{4a}$$

$$m_e n_0 \frac{\partial \mathbf{v}_e}{\partial t} + q_e n_0 \nabla\phi - q_e n_0 \mathbf{v}_e \times \mathbf{B}_0 + m_e v_{te}^2 \nabla n_e = 0, \tag{4b}$$

$$\frac{\partial n_i}{\partial t} + \nabla\cdot(n_0 \mathbf{v}_i) = 0, \tag{4c}$$

$$m_i n_0 \frac{\partial \mathbf{v}_i}{\partial t} + q_i n_0 \nabla\phi + q_i \mathbf{v}_i \times \mathbf{B}_0 + m_i v_{ti}^2 \nabla n_i = 0, \tag{4d}$$

$$\frac{\partial n_\beta}{\partial t} + \nabla\cdot(n_\beta \mathbf{v}_b + n_b \mathbf{v}_\beta) = 0, \tag{4e}$$

$$m_e n_b \frac{\partial \mathbf{v}_\beta}{\partial t} + m_e n_b (\mathbf{v}_b\cdot\nabla)\mathbf{v}_\beta + q_e n_b \nabla\phi - q_e n_b \mathbf{v}_\beta \times \mathbf{B}_0 + m_e v_{tb}^2 \nabla n_\beta = 0, \tag{4f}$$

$$\epsilon_0 \nabla\cdot\nabla\phi = 0. \tag{4g}$$

Nonlinear set

$$\frac{\partial n_e}{\partial t} + \nabla\cdot(n_0 \mathbf{v}_e) = N_e, \tag{5a}$$

$$m_e n_0 \frac{\partial \mathbf{v}_e}{\partial t} + q_e n_0 \nabla\phi - q_e n_0 \mathbf{v}_e \times \mathbf{B}_0 + m_e v_{te}^2 \nabla n_e = \mathbf{F}_e, \tag{5b}$$

$$\frac{\partial n_i}{\partial t} + \nabla\cdot(n_0 \mathbf{v}_i) = N_i, \tag{5c}$$

$$m_i n_0 \frac{\partial \mathbf{v}_i}{\partial t} + q_i n_0 \nabla\phi + q_i \mathbf{v}_i \times \mathbf{B}_0 + m_i v_{ti}^2 \nabla n_i = \mathbf{F}_i, \tag{5d}$$

$$\frac{\partial n_\beta}{\partial t} + \nabla\cdot(n_\beta \mathbf{v}_b + n_b \mathbf{v}_\beta) = N_\beta, \tag{5e}$$

$$m_e n_b \frac{\partial v_\beta}{\partial t} + m_e n_b (\mathbf{v}_b\cdot\nabla)\mathbf{v}_\beta + q_e n_b \nabla\phi - q_e n_b \mathbf{v}_\beta \times \mathbf{B}_0 + m_e v_{tb}^2 \nabla n_\beta = \mathbf{F}_\beta, \tag{5f}$$

$$\epsilon_0 \nabla\cdot\nabla\phi = -q_e(n_e + n_\beta) - q_i n_i, \tag{5g}$$

where

$$N_s = -\nabla\cdot(n_s \mathbf{v}_s),$$
$$\mathbf{F}_s = -m_s n_{s0}[(\mathbf{v}_s\cdot\nabla)\mathbf{v}_s + \tfrac{1}{2}\gamma(v_{ts}^2/n_{s0}^2)\nabla(n_s n_s)], \tag{6}$$

and $s = e$, i, or β for each species. In keeping with the usual expansions consistent to first order, we have written the nonlinear terms which appear as first-order products as source terms on the right-hand side of the Eqs. (5a)–(5f).

We look for normal mode solutions to Eqs. (4) and (5) of the schematic form $x_M = X_M \exp(j\tilde{\omega}_M t - j\mathbf{k}_M\cdot\mathbf{r})$, where x_M represents any plasma variable, and expect two distinct sets of solutions corresponding to the linear and nonlinear sets of equations. For the linear equations the modes exist independent of one another, so that the set of solutions to these equations have the form:

$$\begin{bmatrix} n_{eL}(\mathbf{r},t) \\ \mathbf{v}_{eL}(\mathbf{r},t) \\ n_{iL}(\mathbf{r},t) \\ \mathbf{v}_{iL}(\mathbf{r},t) \\ n_{\beta L}(\mathbf{r},t) \\ \mathbf{v}_{\beta L}(\mathbf{r},t) \\ \phi_L(\mathbf{r},t) \end{bmatrix} = \begin{bmatrix} \tilde{N}_{eM}(\omega_M, \mathbf{k}_M) \\ \mathbf{V}_{eM}(\omega_M, \mathbf{k}_M) \\ \tilde{N}_{iM}(\omega_M, \mathbf{k}_M) \\ \mathbf{V}_{iM}(\omega_M, \mathbf{k}_M) \\ \tilde{N}_{\beta M}(\omega_M, \mathbf{k}_M) \\ \mathbf{V}_{\beta M}(\omega_M, \mathbf{k}_M) \\ \tilde{\Phi}_M(\omega_M, \mathbf{k}_M) \end{bmatrix} \exp(j\Lambda_M \pm \gamma_M t), \tag{7}$$

where $\Lambda \equiv \omega_M t + \mathbf{k}_M\cdot\mathbf{r}$, and $\gamma_M > 0$ represents the linear growth or decay rate of any mode M. Note that due to the linear beam-plasma instability the exponential growth of the conjugate modes ($\gamma_G = -\gamma_D \equiv \gamma$) occurs even in the absence of dissipation and must therefore be explicitly accounted for in the normal mode form. The oscillatory behavior of modes D and G are identical so that we may write $\Lambda_G = \Lambda_D \equiv \Lambda_B$.

The linear form of the equations determine the dispersion relation (1) for the system and may be used to evaluate the expression for the energy of the normal modes which are given by $\mathfrak{D}(\omega, k) = 0$. Simplified expressions for these quantities can be obtained if one assumes

$v_{tb} = v_{ti} = 0$ and studies the usual confined-flow case of $B_0 \to \infty$. Both conditions can be shown to approximate the experimental conditions well. The dispersion relation is then given by

$$\mathfrak{D}(\omega, k) = \frac{k^2}{k_z^2} - \frac{\omega_{pe}^2}{\omega^2}\left(\frac{1}{T_{eB}} + \mathfrak{M} + \frac{\eta}{\left(1 - \frac{v_b}{v_B}\right)^2}\right) = 0, \qquad (8)$$

where $T_{eB} \equiv 1 - \alpha_{te}^2/v_B^2$, $\mathfrak{M} \equiv m_e/m_i$, $\eta \equiv n_b/n_0$, and $v_B \equiv \omega_B/k_{zB}$ is the phase velocity of mode B along the magnetic field axis.

The linear equations are used later to simplify the expressions obtained for the coupling coefficient by relating the seven normal mode amplitudes to a single variable. For example, in terms of the field-induced electron velocity V_{eM}, one finds from the simplified linear equations that

$$\begin{aligned}
&V_{iM} = -\mathfrak{M} T_{eM} V_{eM}, \quad N_{eM} = n_0 \frac{V_{eM}}{v_M}, \\
&V_{BM} = \frac{\omega_M}{\omega_{DM}} T_{eM} V_{eM}, \quad N_{BM} = \frac{n_b \omega_M k_{zM}}{\omega_{DM}^2} T_{eM} V_{eM}, \qquad (9) \\
&\Phi_M = \frac{m_e}{q_e} v_M T_{eM} V_{eM}, \quad N_{iM} = -\frac{n_0}{v_M} \mathfrak{M} T_{eM} V_{eM}, \\
&E_M = j \frac{m_e}{q_e} \frac{\omega_M}{k_{zM}} k_M T_{eM} V_{eM},
\end{aligned}$$

where $\omega_{DM} = \omega_M - v_b k_{zM}$. The linear equations also provide several useful properties of the normal mode amplitudes which can be used to relate the four coupling coefficients that are obtained independently for each of the interacting waves. Arbitrarily choosing V_{eM} to be real and taking the rest of the variables to be complex, we can show from (9) that $V_{eD} = V_{eG}$. Similarly, one can show for the equations describing this experiment that the normal mode amplitudes X_M of the conjugate waves D and G satisfy the relation $X_D = X_G^*$, where the asterisk denotes the complex conjugate.

For the nonlinear set of equations, the solutions are coupled by the nonlinear interactions which give rise to s slowly-varying amplitude $a_M(\mathbf{r}, t)$ which is identical for each variable. The set of nonlinear solutions to Eqs. (5) may therefore be written:

$$\begin{bmatrix} n_{eN}(\mathbf{r},t) \\ \mathbf{v}_{eN}(\mathbf{r},t) \\ n_{iN}(\mathbf{r},t) \\ \mathbf{v}_{iN}(\mathbf{r},t) \\ n_{BN}(\mathbf{r},t) \\ \mathbf{v}_{BN}(\mathbf{r},t) \\ \phi_N(\mathbf{r},t) \end{bmatrix} = \sum_M \begin{bmatrix} \tilde{N}_{eM}(\omega_M, \mathbf{k}_M) \\ \tilde{\mathbf{V}}_{eM}(\omega_M, \mathbf{k}_M) \\ \tilde{N}_{iM}(\omega_M, \mathbf{k}_M) \\ \tilde{\mathbf{V}}_{iM}(\omega_M, \mathbf{k}_M) \\ \tilde{N}_{BM}(\omega_M, \mathbf{k}_M) \\ \tilde{\mathbf{V}}_{BM}(\omega_M, \mathbf{k}_M) \\ \tilde{\Phi}_M(\omega_M, \mathbf{k}_M) \end{bmatrix} a_M(\mathbf{r}, t) \exp(j\Lambda_M \pm \gamma_M t), \qquad (10)$$

where the sum is over the interacting modes. We assume that the interaction is resonant so that

$$\begin{aligned}
&\omega_D = \omega_G \equiv \omega_B = \omega_A + \omega_T, \qquad (11) \\
&\mathbf{k}_D = \mathbf{k}_G \equiv \mathbf{k}_B = \mathbf{k}_A + \mathbf{k}_T.
\end{aligned}$$

Only the resonant combinations of modes defined by these matching conditions are allowed to contribute to the evolution of the modes in Eq. (10).

To derive a conservation equation from the set of equations (4) and (5), we follow the generalized approach of Bers and Penfield.[8] The equations are multiplied by the necessary quantities and added or combined until all terms reduce to a time-derivative or divergence of some quantity, as in Eq. (3). The nonlinear terms combine to constitute the external driving term p_e. By setting the nonlinear terms to zero, the remaining quantities can be identified as the small-signal energy and power flow and can be evaluated accordingly for any mode. Using the subscripts L and N to denote the linear and nonlinear equations and solutions, we form the quantity:

$$\begin{aligned}
&[(\mathbf{v}_{eN} \cdot 4b) + (\mathbf{v}_{iN} \cdot 4d) + (\mathbf{v}_{BN} \cdot 4f)] \\
&+ [\mathbf{v}_{eL} \cdot 5b) + (\mathbf{v}_{iL} \cdot 5d) + (\mathbf{v}_{BL} \cdot 5f)]. \qquad (12)
\end{aligned}$$

Equations (4a), (4c), (4e) and (5a), (5c), (5e) can be used to form the relations

$$\nabla \cdot \mathbf{j}_{tN} = \sum_s q_s N_s, \quad \nabla \cdot \mathbf{j}_{tL} = 0, \qquad (13)$$

where $\mathbf{j}_t \equiv \mathbf{j}_p - \epsilon(\partial/\partial t)\nabla\phi$ is the total current and $\mathbf{j}_p \equiv \sum_s q_s n_{s0} \mathbf{v}_s + q_e \mathbf{v}_b n_B$ is the particle current. Using these and the beam force equation, we obtain:

$$\begin{aligned}
&\frac{\partial}{\partial t}\left(\sum_s m_s n_{s0} \mathbf{v}_{sN} \cdot \mathbf{v}_{sL} + \sum_s \frac{m_s v_{ts}^2}{n_{s0}} n_{sN} n_{sL} + \epsilon_0 \nabla\phi_N \cdot \nabla\phi_L \right. \\
&\left. + n_{BN} T_L + n_{BL} T_N\right) + \nabla \cdot \left[\sum_s m_s v_{ts}^2 (n_{sL} \nabla_{sN} + n_{sN} \nabla_{sL}) \right. \\
&\left. + \mathbf{j}_{tN}\phi_L + \mathbf{j}_{tL}\phi_N + \frac{T_L \mathbf{j}_{bN}}{q_e} + \frac{T_N \mathbf{j}_{bL}}{q_e} + \frac{2 m_e v_{tb}^2}{n_b} n_{BN} n_{BL} \nabla_b\right] \\
&= \sum \mathbf{v}_{sL} \cdot \mathbf{F}_s + \sum_s m_s v_{ts}^2 \frac{n_{sL}}{n_{s0}} N_s + \phi_L \sum_s q_s N_s \\
&+ \mathbf{v}_b \cdot \frac{n_{BL} \mathbf{F}_b}{n_b} + T_L N_b, \qquad (14)
\end{aligned}$$

where $\mathbf{j}_b \equiv q_e(n_B \mathbf{v}_b + n_b \mathbf{v}_B)$ is the beam current and $T_L \equiv m_e \mathbf{v}_B \cdot \mathbf{v}_b$. Here, we have again assumed the confined-flow limit to eliminate vector cross-product terms which otherwise appear on the right-hand side of (14) and cannot be physically interpreted as either mode energy or power flow.

B. Derivation of the coupled-mode equations

The form of the terms on both sides of Eq. (14) is suggestive of a coupled-mode equation. Each term on the left-hand side involves the product of a linear and nonlinear solution, while each term on the right-hand side involves the product of two nonlinear and a linear solution. When the normal mode form of the solutions is substituted into Eq. (14), each term on the left-hand side will contribute a single slowly varying amplitude, while the right-hand side will contribute a product of slowly varying amplitudes. The modes associated with each of the solutions are then chosen to satisfy the resonance conditions.

For example, consider the following terms from the conservation equation just derived:

$$\frac{d}{dt}(m_e n_0 \mathbf{v}_{eN}\cdot\mathbf{v}_{eL}+\dots) = -q_e\phi_L\nabla\cdot(n_{eN}\mathbf{v}_{eN})+\dots . \quad (15)$$

Again, schematically writing any of the plasma variables $x = n$, v, or ϕ as $x = a_M X_M \exp(j\Lambda_M)$, we obtain a coupled-mode equation for a stable mode (say, mode A) by taking:

$$x_N = a_A X_A \exp(j\Lambda_A) + a_T X_T \exp(j\Lambda_T) + [a_G X_G \exp(\gamma t) + a_D X_D \exp(-\gamma t)]\exp(j\Lambda_B) \quad (16)$$

$$x_L = X_A^* \exp(-j\Lambda_A).$$

The left-hand side of Eq. (15) then becomes

$$\frac{d}{dt}\{m_e n_0[a_A V_{eA}\exp(j\Lambda_A) + a_T V_{eT}\exp(j\Lambda_T)+\dots] \times [V_{eA}^*\exp(j\Lambda_A)]+\dots\} = \frac{d}{dt}[a_A(|V_A|^2+\dots)] = \frac{d}{dt}(a_A w_A), \quad (17)$$

where w_A has been identified as the small-signal wave energy given as usual by a sum of terms of the form $X_A X_A^* = |X_A|^2$. In the absence of any nonlinear terms ($p_e - 0$), therefore, Eq. (14) reduces to a statement of the constancy of wave energy for a stable mode:

$$(d/dt)(w_A) = 0. \quad (18)$$

When $p_e \neq 0$, however, the nonlinear terms of (15) becomes

$$[\Phi_A^*(\exp -j\Lambda_A)]\nabla\cdot[a_T^* N_{eT} a_B \mathbf{V}_{eB}\exp(-j\Lambda_T + j\Lambda_B)] = \{\Phi_A^*\exp(-j\Lambda_A)(-jk_A)\exp(j\Lambda_A)N_{eT}^* V_{eB}\} a_T^* a_B \quad (19)$$

so that w_A can be factored out, using (18), to obtain the desired coupled-mode equation

$$w_A(d/dt)a_A = p_{e,A} = K_A a_T^* a_B. \quad (20)$$

For an unstable wave (mode D or G) the modal energy changes on a time scale $\gamma^{-1} > \omega^{-1}$, so that (18) is not true and a different form for modal energy must be adopted. If we attempt to derive an equation for a_G in a similar manner, we would let each system variable take the form

$$x_N = a_G X_G \exp(j\Lambda_B + \gamma t) + a_D X_D \exp(j\Lambda_B + \gamma t) + \dots ,$$

$$x_L = X_G^* \exp(-j\Lambda_B + \gamma t). \quad (21)$$

For this case, it is not possible to both satisfy the resonance conditions and obtain an expression for model energy of the form $|E_G|^2$. The exponential factors do not fully cancel, and Eq. (14) becomes

$$(d/dt)[w_G \exp(2\gamma t)] = 0. \quad (22)$$

Since both the differential operator and the exponential factor involve the slow time scale variation, in the limit $p_e - 0$ we are forced to conclude that $w_G = 0$ so that a coupled-mode equation for a_G cannot be obtained. However, from Eq. (21) it can be seen that both the oscillatory and exponential behavior will cancel when the product involving $a_D X_D X_G^*$ is taken. In fact, this is the only contributing product and yields a form for the modal "energy" (now that for the total beam-plasma mode) which is given by a sum of terms $\sum X_D X_G^* \sim E_D E_G^*$ and can be shown to be a constant quantity using the linear equations. From this formalism, one therefore obtains a coupled-mode equation for a_D of the form

$$\frac{d}{dt}[a_D(V_{eD}V_{eG}^*+\dots)] = \tilde{w}_B\frac{d}{dt}a_D = K_D a_A a_T. \quad (23)$$

In analogy with the expression obtained for stable modes, we are therefore led to define a new quantity (within the parenthesis) for the energy of the beam-plasma mode which we shall denote $\tilde{w}_B$. It cannot be energy in the usual sense, since, in general, it is a complex quantity and involves a part of both the decaying and growing beam-plasma mode. This form for $\tilde{w}_B$ is of the type usually obtained after introducing the mathematical concept of adjoint field quantities in connection with rapidly decaying waves, but here the concept has a more physical basis in the presence of the decaying and growing fields which comprise the total beam-plasma mode.[9]

The physical interpretation of the beam-plasma energy is made clearer by evaluating the expressions for $\tilde{w}_B$ and $\tilde{s}_{zB}$ consistently with the confined-flow dispersion relation given in Eq. (8). Using the simplified linear equations to express the mode amplitudes in terms of E_M and derive the dispersion relation, one can show that

$$\tilde{w}_B = \epsilon_0 E_D E_G^* \omega \frac{\partial}{\partial\omega}\mathfrak{D}\Big|_{\tilde{\omega}_B}, \quad \tilde{s}_{zB} = \epsilon_0 E_D E_G^* \omega \frac{\partial}{\partial k_z}\mathfrak{D}\Big|_{\tilde{\omega}_B}. \quad (24)$$

Thus, $\tilde{w}_B$ is still given by the usual expression for mode energy, but it must now be evaluated at the complex root $\tilde{\omega}_B$, rather than at the real root as for the case of a stable mode. Later analysis will also show that the nonlinear stability and saturated amplitude of the beam mode depends on the physically more-meaningful sign parity of the real part of $\tilde{w}_B$.[3,10]

An equation for the behavior of the growing beam-plasma mode, similar to Eq. (23), may be found in the same way as that for a_D and involves its own form for the coupling coefficient. This coefficient and those obtained for a_A and a_T, can then be related to that obtained in the equation for a_D by using the symmetry relations between the normal mode amplitudes which were discussed earlier. This is tantamount to deriving Manley–Rowe relations for the parametric interaction and permits the coupled mode equations for the four modes to be written in terms of a single coupling coefficient, as we show in the next section.

C. Coupling coefficient and symmetry relations

To derive an expression for the coupling coefficient, we proceed to evaluate the right-hand side of Eq. (14) in the limit where $v_{ti} = v_{th} = 0$ and $B_0 - \infty$, and find

$$\mathbf{v}_{eL}\cdot\mathbf{F}_e + \mathbf{v}_{iL}\cdot\mathbf{F}_i + \mathbf{v}_{\beta L}\cdot\mathbf{F}_\beta + \phi_2[q_e(N_e+N_\beta)+q_i N_i] + \frac{m_e v_{te}^2}{n_0} n_{eL} N_e + \frac{n_{\beta L}}{n_b}\mathbf{v}_b\cdot\mathbf{F}_b + m_e\mathbf{v}_b\cdot\mathbf{v}_{\beta L}N_b. \quad (25)$$

In the equation describing the growing beam-plasma mode $a_G(r,t)$, we recognize which products will contribute to the nonlinear driving term by taking

$$x_L \sim X_D^*\exp(-j\Lambda_B - \gamma t), \quad x_N \sim a_G X_G \exp(j\Lambda_B + \gamma t),$$

so that both exponential and oscillatory variations will cancel under the assumed matching conditions. After substituting this into Eq. (14) and normalizing the nor-

mal mode amplitudes to the field-induced electron velocity, one finds

$$(d/dt)a_G = jm_e n_0 V_{eA} V_{eT} V_{eB} e^{\gamma t} K_B^* (\tilde{\omega}_B^*/\tilde{w}_B^*) a_A a_T .$$

Here, the coupling coefficient is given by

$$\tilde{K}_B^* = \left[\left(\frac{1}{v_A}+\frac{1}{v_T}+\frac{1}{v_B^*}\right)+\frac{\alpha_{te}^2}{v_A v_T v_B^*}\right]-\mathfrak{M}^2 T_A T_T T_B^*\left(\frac{1}{v_A}+\frac{1}{v_T}+\frac{1}{v_B^*}\right)$$
$$+\frac{\eta T_A T_T T_B^*}{\left(1-\frac{v_b}{v_A}\right)\left(1-\frac{v_b}{v_T}\right)\left(1-\frac{v_b}{v_B^*}\right)}\left(\frac{1}{v_A-v_b}+\frac{1}{v_T-v_b}+\frac{1}{v_B^*-v_b}\right). \tag{26}$$

Equations for the other mode amplitudes are found similarly. To obtain a coupled-mode equation for the decaying beam-plasma mode, for example, we evaluate the same expressions after taking

$$x_L \sim X_G^* \exp(-j\Lambda_B+\gamma t), \quad x_N \sim a_D X_D \exp(j\Lambda_B-\gamma t).$$

To obtain equations for the stable A and T modes, we must allow both the decaying and growing beam-plasma mode to act as pumps in conjunction with the remaining stable mode. For example, one of the nonlinear terms in Eq. (25), $q_e\phi_L \nabla\cdot(n_{eN}\mathbf{v}_{eN})$, takes the following form when evaluating the coupled mode equation for mode A:

$$q_e\phi_A^* \exp(-j\Lambda_A)[-jk_A][a_D N_{eB}\exp(-\gamma t)+a_G N_{eB}^* \exp(\gamma t)]$$
$$\times \exp(j\Lambda_B) a_T^* V_{eT}^* \exp(-j\Lambda_T)+[a_D V_{eB}\exp(-\gamma t)$$
$$+a_G V_{eB}^* \exp(\gamma t)]\exp(j\Lambda_B - j\Lambda_T) a_T^* N_{eT}^* .$$

In this expression the nonlinear term involving the density and velocity products has been properly symmetrized with respect to variations at Λ_A and Λ_T, as required by the matching conditions.

The resulting four coupled-mode equations can be simplified and the exponential growth and decay factors eliminated by normalizing the mode amplitudes to the action density

$$A_M \equiv a_M (w_M/\omega_M)^{1/2} \exp(\gamma_M t). \tag{27}$$

We then find that the coupled-mode equations may be written as

$$\left(\frac{d}{dt}+\gamma\right)A_D = jKA_A A_T, \quad \left(\frac{d}{dt}-\gamma\right)A_G = jK^* A_A A_T,$$
$$\frac{d}{dt}A_A = jA_T^*(KA_D+K^*A_G), \quad \frac{d}{dt}A_T = jA_A^*(KA_D+K^*A_G), \tag{28}$$

where d/dt again represents the convective derivative. Here, symmetry relations which exist between the four coupling coefficients have been used to write the four equations in terms of a single coefficient. Equation (26) can also be further simplified by using the following ordering of system parameters which correspond to experimental conditions of interest (see Fig. 1):

$$v_A \gg v_b, \quad v_B \lesssim v_b, \quad v_b \gg v_{te}, \quad v_B \approx -v_T \approx v_b .$$

The simplified coefficient is then given by

$$\tilde{K} = \frac{\omega_{pe}}{2v_A}\frac{k_A}{k_{sA}}\left(\frac{\mathfrak{M}}{2}\frac{\omega_A}{\omega_T}\frac{\omega_B}{m_e n_0}\right)^{1/2}\frac{\omega_{pe}}{k_B v_B}\frac{1}{\tilde{U}_B^{1/2}}. \tag{29}$$

The complex phase angle of $\tilde{K}$ is determined primarily by the complex factor $\tilde{U}_B^{1/2}$, which arises from the energy of the beam-plasma mode given by Eq. (24):

$$\tilde{U}_B^{1/2} = \frac{1}{\tilde{T}_B^{1/2}}+\mathfrak{M}-\eta\left(\frac{\tilde{v}_B}{v_b}\right)^3\left(1-\frac{\tilde{v}_B}{v_b}\right)^{-3}. \tag{30}$$

The symmetry between the coupling coefficient can also be shown to satisfy Manley–Rowe relations describing energy flow between the modes. Equations (28) can be combined to obtain

$$\frac{d}{dt}|A_A|^2 = \frac{d}{dt}|A_T|^2 = -\frac{d}{dt}2R_e(A_D A_G^*).$$

It follows from Eq. (27) that the slow variations in mode energies are given by

$$\left|\frac{\Delta\tilde{w}_B}{\Delta w_T}\right| = -\left|\frac{\omega_B}{\omega_T}\right|; \quad \left|\frac{\Delta w_T}{\Delta w_A}\right| = \left|\frac{\omega_T}{\omega_A}\right|.$$

The energy flow is therefore from the beam-plasma mode into modes A and T in the ratio of their frequencies.

Threshold effects for this interaction can be studied by assuming a strong undepleted pump mode. The relevant coupled-mode equations for the driven modes are then

$$\frac{d}{dt}A_A = jK^* A_T^* A_B, \quad \frac{d}{dt}A_T = jK^* A_A^* A_B,$$

where K^* is the coupling coefficient derived previously. Assuming that modes A and T have exponential variations with damping rates ν_A and ν_T, respectively, at instability threshold we have

$$\frac{V_{eB}^2}{v_{te}^2} > 16\frac{\nu_A\nu_T}{\omega_A\omega_T}\left[1-\frac{\eta}{2}\frac{v_{te}^2}{v_b^2}\left(1-\frac{v_b}{v_B}\right)^{-2}\right]^{-1/2},$$

where V_{eB} is the field-induced electron velocity. In the limit $\eta \to 0$ this reduces to the usual result involving the decay of an electron plasma wave into another electron plasma wave and an ion-acoustic wave.

Equation (30) shows that the magnitude and phase of the coupling coefficient is most sensitive to the beam term in $\tilde{U}_B^{1/2}$. For weak beam-plasma interactions, where $v_B \approx v_b$, $|K|$ will be small and the wave-wave coupling correspondingly weak. For stronger beam-plasma interactions, however, where the difference between the beam drift velocity and phase velocity of the beam-plasma mode becomes appreciable, the coupling coefficient can be significantly enhanced. This difference depends sensitively upon several system parameters and will be discussed in detail shortly.

In the work to follow, it is convenient to rewrite the coupled mode equations in terms of dimensionless quantities. We choose to normalize all mode amplitudes to the initial value of mode A [denoted as $A_{A0} = A_A(0)$] and to scale other parameters accordingly:

$$\left(\frac{\partial}{\partial\tau}+\frac{\partial}{\partial x}+\Gamma\right)\tilde{D} = j\exp(j\theta_K)\tilde{A}\tilde{T},$$
$$\left(\frac{\partial}{\partial\tau}+\frac{\partial}{\partial x}-\Gamma\right)\tilde{G} = j\exp(-j\theta_K)\tilde{A}\tilde{T}, \tag{31}$$
$$\left(\frac{\partial}{\partial\tau}+\frac{v_{gA}}{v_{gB}}\frac{\partial}{\partial x}+\Gamma_a\right)\tilde{A} = j\tilde{T}^*[\tilde{D}\exp(j\theta_K)+\tilde{G}\exp(-j\theta_K)],$$
$$\left(\frac{\partial}{\partial\tau}+\frac{v_{gA}}{v_{gB}}\frac{\partial}{\partial x}+\Gamma_t\right)\tilde{T} = j\tilde{A}^*[\tilde{D}\exp(j\theta_K)+\tilde{G}\exp(-j\theta_K)],$$

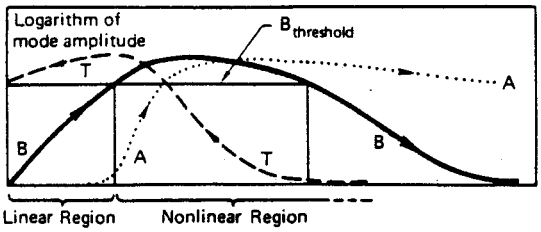

FIG. 3. Anticipated behavior for the nonlinear evaluation of the beam-plasma instability.

where

$$\tau \equiv |K||A_{A0}|t; \quad x \equiv \frac{|K||A_{A0}|}{v_{gB}} z,$$

$$\Gamma \equiv \frac{\gamma}{|K||A_{A0}|}; \quad M \equiv \frac{A_M(x,\tau)}{|A_{M0}|}.$$

Here, the coupling coefficient has been written in terms of its magnitude and phase $\bar{K} = |K| \exp(j\theta_K)$, and $v_{gM} \equiv \partial\omega/\partial k_z|_M$ carries sign parity so that $v_{gT} < U$. For generality, we have included the effect of linear damping of the plasma modes.

The most striking difference between Eqs. (31) and the usual three-wave model is that for this case the coupling coefficient is, in general, a complex quantity, instead of being purely real. The manner in which $|K|$ and θ_k appear in the equations indicates that the magnitude of the coupling coefficient determines only the rate of the nonlinear mode evolution, while its phase [and therefore that of $\tilde{w}_B^{1/2}$ in Eq. (30)] determines the stability of the interaction.

III. SOLUTIONS TO THE STEADY-STATE EQUATIONS

Equations (31) describe the early nonlinear evolution of the system where first-order corrections to the linear instability occur. To properly describe the spatial mode profile which is observed experimentally, Eqs. (31) should exhibit the qualitative behavior shown in Fig. 3. An extended region of linear behavior exists where the beam-plasma and plasma modes independently propagate at unperturbed growth or decay rates. The amplitude of the beam-plasma mode eventually reaches a threshold pump level for parametric decay where modes A and T grow at the expense of the energy of mode B. If the dynamics permit, the energy loss will stabilize the linear growth of mode B and the system will thereafter exhibit fully nonlinear behavior. For a system of finite length $\mathcal{L}$, mode T must grow from thermal levels near the end of the system. On a longer space scale, therefore, mode B must either decay to below threshold levels or higher-order processes will occur which decouple the modes.

To obtain the time-asymptotic spatial profile predicted by Eqs. (31), a complete space-time solution to the set of partial differential equations is required. In general, the special cases involving the time-independent ($d/dt = 0$) or space-independent ($d/dx = 0$) equations cannot be expected to reveal the exact final state of the system. An analysis of the three-wave analog to this problem has shown that, although periodic steady-state solutions to the time-independent case can be found, the system will always evolve into a unique spatial state which exhibits decaying long-term behavior for all three modes and is otherwise accessible by only a specific set of boundary conditions.[11,12]

We have therefore initially chosen to investigate the more limited question of system stability by considering the early nonlinear behavior predicted by the steady-state time and space equations independently. Parameter sensitivity studies are made for each case to verify the numerical and analytical results. At the same time, the scaling laws obtained from these sensitivity studies span the large parameter space which is covered by the four-wave system, identify sensitive system parameters, and predict behavior which can be compared with that observed experimentally. Common behavior for the two special cases may also be indicative of that for the exact space-time solution.

The normal mode amplitudes used for initial or boundary conditions have been calculated using a fluctuation-dissipation theorem relevant to the experimental conditions of interest here.[5] The initial mode amplitudes are assumed to arise from beam or plasma fluctuations prior to the linear coupling, when the usual statistical methods may be used. The dressed test-particle approach may be used to calculate the wavenumber spectrum for any mode M[13]

$$\langle E_{k_z}^2 \rangle_M = \frac{F_g}{2\pi\epsilon_0} \frac{\sum_s q_s^2 n_s f_s(v_{gM})}{\sum_s (\omega_M/\lambda_{D_s}^2) f_s(v_{gM})} \frac{1}{\frac{\partial}{\partial\omega}\mathcal{K}_R\Big|_M}$$

where $F_g^{-1} \approx a^2 J_1^2(k_{10}a)$, a is the plasma radius, f_s is the Maxwellian distribution, λ_{D_s} is the Debye length of each species, and $\mathcal{K}_R$ is the real part of the dielectric tensor. The thermal field strength for each mode can then be evaluated by integrating this expression over self-consistent matching regions in (ω, k) space. This has been done for both an unmodulated beam and where the beam energy has been entrained above thermal levels over a narrow bandwidth. The initial conditions calculated for these cases are summarized in Table I. It can be seen that the nonthermal beam fluctuations dominate the modulated case as expected. More importantly, the normalized linear growth rate Γ is found to be a large parameter in this system of equations, and this fact can be exploited to obtain asymptotic solutions for the mode behavior.

Equations (31) have been investigated analytically for the time- and space-independent cases within certain limits where solutions are possible and scaling laws can

TABLE I. Initial conditions for the cases of a modulated and an unmodulated beam.

	Unmodulated	Modulated
Λ_0	1	1
T_0	0.17	0.15
B_0	0.02	3.8
Γ	5.6×10^6	4.0×10^{10}

be obtained. The equations have also been integrated numerically using a linear multi-step predictor-corrector package, with conservation conditions derived from the relevant equations evaluated at each step to insure that the integration proceeds accurately. The equations have been integrated using the rectangular form for the complex mode amplitude to avoid the singular behavior which occurs in the limit $A_{A0}=0$, a case of interest when studying the three-wave analog to this problem.

A. The space-independent equations

The simplest case of this four-wave interaction is obtained by considering coupling of the modes in time only. For this case, it is not possible to demonstrate nonlinear system stability directly by standard phase-space arguments or by deriving constants of the motion. The two independent motion constants which can be derived

$$\frac{d}{dt}[|A|^2-|T|^2]=0, \tag{32a}$$

$$\frac{d}{dt}[|A|^2+2\mathrm{Re}(DG^*)]=0, \tag{32b}$$

do not show boundedness of any mode solutions, but can be used to determine the accuracy of the numerical integration and to simplify the form of the coupled mode equations. If modes A and T are assumed equal at any time (say $t=0$), then by Eq. (32a) they will remain equal for subsequent times, and one equation can be eliminated. In addition, if modes D and G are combined and written as a single beam-plasma mode (denoted by B), we find the problem can be reduced to one involving only two variables:

$$\begin{aligned}&\frac{d^2}{dt^2}B+[4\mathcal{W}|A|^2-\Gamma^2]B=j2\Gamma\mathfrak{X}A,\\&\frac{d}{dt}A=A^*B,\end{aligned} \tag{33}$$

where $\mathcal{W}\equiv\cos(2\theta_k)\sim\mathrm{Re}(\tilde{w}_B)$, $\mathfrak{X}\equiv\sin(2\theta_k)$, and $B\equiv j[D\exp(j\theta_K)+G\exp(-j\theta_K)]$. The sign of $\mathcal{W}$ is obviously the dominant factor in determining system stability, and may be regarded as the sign parity of the "total" beam-plasma mode energy. Additionally, with the usual assumed condition of phase-locked modes, one can obtain the following form for Eq. (33):

$$\begin{aligned}&\frac{d^2}{d\tau^2}b(\tau)+(4\mathcal{W}a^2-\Gamma^2)b+2\Gamma\mathfrak{X}c_0=0,\\&a(\tau)=\cosh^{1/2}\left[2\int_0^\tau b(t)dt\right],\end{aligned} \tag{34}$$

where a, b are the magnitude of modes A and B, and c_0 is a constant factor. A linear regime clearly exists initially where $\Gamma^2\ll 4\mathcal{W}a^2$. As mode A is driven nonlinearly, a turning point is reached for mode B if $\mathrm{Re}(\tilde{w}_B)>0$, while enhanced growth occurs for $\mathrm{Re}(\tilde{w}_B)<0$. The constant term is small over most of the range and serves only to determine precisely where $(d^2/dt^2)b$ vanishes.

The existence of a turning point can be seen for the special case $\mathfrak{X}\equiv 0$ by defining $u(\tau)=\int_0^\tau b(t)dt$. Integrating Eq. (34) twice gives

$$\int_0^\tau dt=\int_0^{u(\tau)}[P(u)]^{-1/2}du, \tag{35}$$

where $P(u)=\Gamma^2u^2-2\mathcal{W}\cosh(2u)+C_2$, and $C_2=2+[(d/dt)u]^2>2$.

The roots of $P(u)$ determine the behavior of $u(\tau)$. For $\mathcal{W}>0$, two distinct roots exist, so that near a root u_T we can write $P(u)\sim(u-u_T)$ and Eq. (35) becomes $(\tau-\tau_T)\sim(u_T-u)^{1/2}$. Therefore, a turning point occurs at finite time τ_T and bounded solutions for $b(\tau)$ exist. For negative values of $\mathcal{W}$, a double root in $P(u)$ occurs and Eq. (35) becomes $(\tau-\tau_T)\sim\ln(u-u_T)$. For this case a turning point does not exist for finite τ_T. Although no closed form solution to Eq. (35) could be found, one expects τ_T to scale as Γ^{-1} since $\Gamma\gg 1$.

The fact that Γ is a large parameter also permits one to obtain approximate solutions to Eq. (34) in the linear and turning point regions for $\mathcal{W}>0$. Assume a WKB for $b(\tau)$ which permits either growing or oscillatory behavior

$$b(\tau)=b_0\exp\left[\int_0^\tau\omega(t)dt\right]. \tag{36}$$

In the linear region the equation for $\omega(t)$ obtained from (34) reveals that ω is approximately constant and equals $\pm\Gamma$, so that "linear" solutions for the beam and plasma modes can be written:

$$b(\tau)=b_0\cosh(\Gamma\tau),\quad a=\cosh^{1/2}\left[2\int b(t)dt\right]. \tag{37}$$

As we have shown, the nonlinear growth of the plasma modes cause mode B to reach a turning point where $(d^2/d\tau^2)b=0$. In this region, Eq. (34) has the solution

$$b(\tau)=\alpha^{-2/3}\mathrm{Ai}[\alpha^{1/3}(\tau-\tau_T)], \tag{38}$$

where $\alpha=4\Gamma(da/d\tau)|_{\tau_T}$ and Ai is the Airy function. For $\tau<\tau_T$, Eq. (38) exhibits growing solutions into the turning point, while for $\tau>\tau_T$, $b(\tau)$ exhibits oscillating solutions as it evolves away from the turning point. Asymptotic matches can be shown to exist between the linear and turning point solution, and between the turning point solution and that of the full nonlinear equations.[5] Although these results do not provide explicit solutions to the system of equations, they demonstrate the existence of bounded behavior and stabilized growth as a result of the nonlinear mode coupling.

These results can be verified by comparing the scaling predicted from the appropriate "linear" solutions with those observed from a numerical integration of Eqs. (31). Using Eqs. (37) and the requirement that $4a^2(\tau)=\Gamma^2$ at $\tau=\tau_T$, we can solve for τ_T and the turning point amplitude $b(\tau_T)$:

$$\Gamma\tau_T\approx\ln\left[\frac{\Gamma}{b_0}\ln\left(\frac{\Gamma^2}{2}\right)\right],\quad b\tau_T\approx\Gamma\ln\left(\frac{\Gamma}{\sqrt{2}}\right). \tag{39}$$

Thus, the saturation level of the beam plasma should be insensitive to its initial amplitude and scale approximately linearly with the normalized growth rate Γ.

The space-independent form of Eqs. (31) have been integrated numerically over a variety of system conditions, and typical results are shown in Fig. 4 for sever-

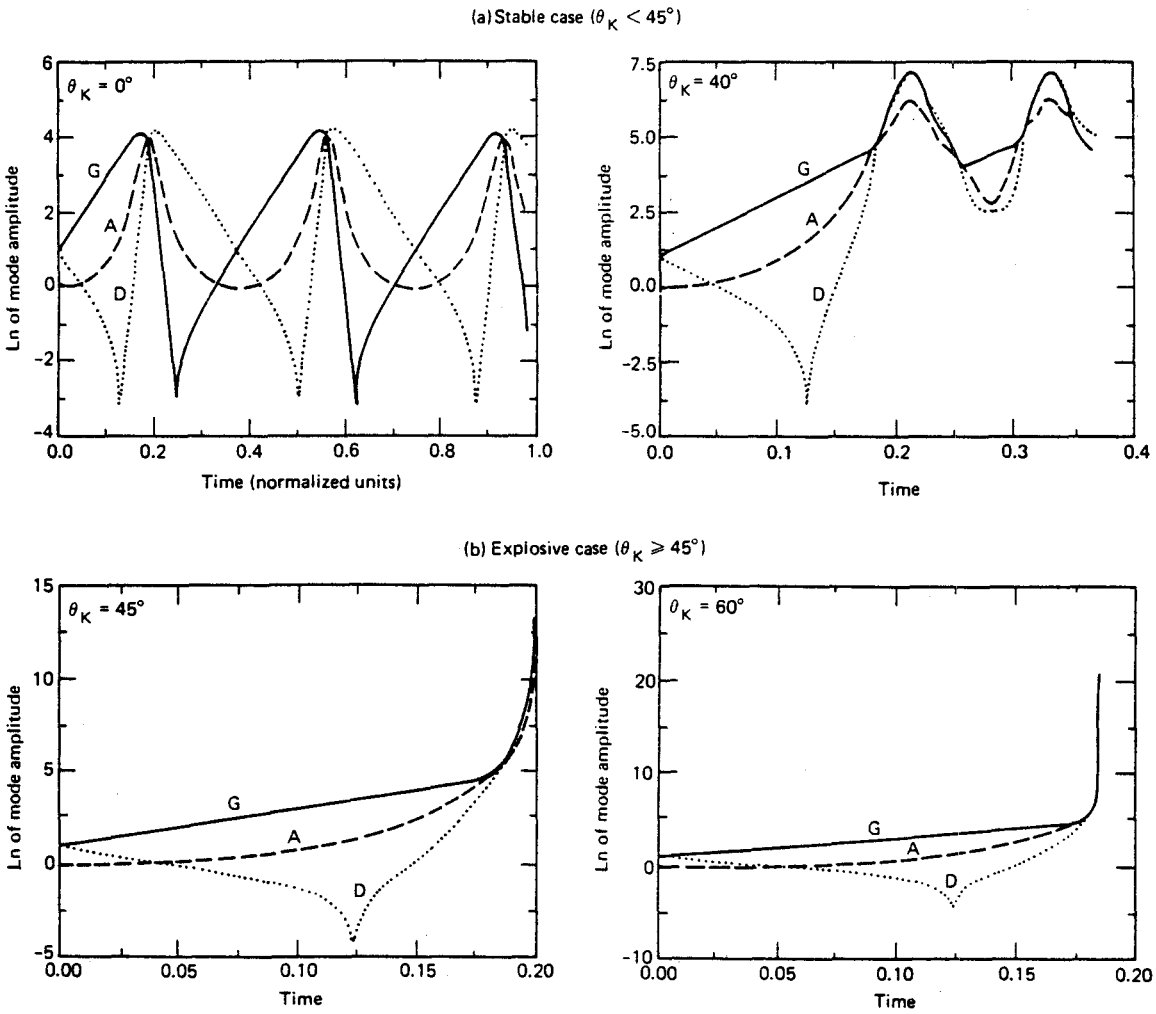

FIG. 4. Time evolution of modes D, G, and A (A = T assumed) for (a) stable, and (b) explosively-unstable cases.

al phase angles of the coupling coefficient. The interaction is stable for $|\theta_k| < 45°$, while explosive behavior occurs for $|\theta_k| \geq 45°$, corresponding to $\mathrm{Re}(\tilde{w}_B) \leq 0$. For $|\theta_k| > 45°$ the explosion point moves to earlier times. A distinct region of linear growth exists for the beam-plasma mode until mode A becomes sufficiently large to couple all four modes. Since mode D reaches amplitudes comparable to the other modes, the interaction must be viewed as a full four-wave coupling. In the fully nonlinear region, the system evolves as a series of bounded relaxation oscillations or exhibits oscillatory behavior. By a systematic variation of parameters the scaling relations predicted by Eqs. (35) and (39) have been verified.[5] One of the most interesting results of these sensitivity studies, however, is the strong dependence of the saturated amplitude $b(\tau_T)$ on the phase angle of the coupling coefficient. This is shown in Fig. 5 where we plot the logarithm of the amplitude of the mode action density versus θ_k. This indicates that the saturation amplitude can span a wide range of values, increasing significantly for $\theta_k \gtrsim 20°$. This suggests that transitional nonlinear behavior is possible. For example, while pump depletion might stabilize the growth of the beam-plasma mode for small values of θ_k other mechanisms could intervene for larger values of θ_k to limit the mode amplitude before pump depletion can occur.

B. The time-independent equations

An analysis of the steady-state spatial equations is substantially more complex than the previous case, since the interaction now involves a backward traveling mode and the problem becomes a boundary-value problem, rather than an initial-value problem. Mode T must grow from thermal levels at the end of the system, so that numerical integration of the equations now requires a variation of T ($x = 0$) to satisfy T ($x = \mathcal{L}$) ≈ 0.

We again find it convenient to combine modes D and G into a single mode B to obtain

$$\frac{d^2}{dx^2}B + [2w(C_1|T|^2 - C_2|A|^2) - \Gamma^2]B - 2wAT(C_1\Gamma_a - C_2\Gamma_t) = j2\Gamma wAT,$$

$$\frac{d}{dx}A = -C_1(\Gamma_a A - T^*B), \quad \frac{d}{dx}T = C_2(\Gamma_t T - A^*B),$$

where all variables are defined as in Eqs. (33), and the constants $C_1 \equiv v_{gB}/v_{gA} \gg 1$ and $C_2 \equiv v_{gB}/|v_{gT}| \lesssim 1$. We have explicitly taken $v_{gT} < 0$ in these equations. If we set $\Gamma_a = \Gamma_t = 0$ as before, conserved quantities can be derived which require periodic behavior for modes A and T:

$$\frac{d}{dx}[C_1|T|^2 + C_2|A|^2] = 0,$$

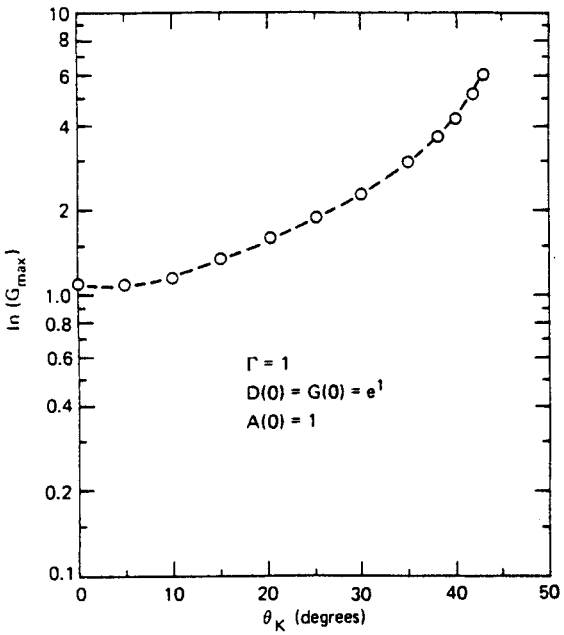

FIG. 5. Saturation amplitude of beam plasma wave versus phase angle of coupling coefficient for space-independent equations.

$$\frac{d}{dx}\left[2C_1\,\mathrm{Re}(DG^*)+|A|^2\right]=0\,.$$

Since C_1, $C_2>0$, this requirement of bounded solutions shows that the mode coupling cannot have a destabilizing effect on the beam-plasma instability; at the same time, it does not insure that linear growth of the beam-plasma mode will saturate by pump depletion.

The simplified phase-locked equations for this case can again be used to predict the early nonlinear system behavior

$$\frac{d^2}{dx^2}b+[2(C_1t^2-C_2a^2)-\Gamma^2 b]=2at(c_1\Gamma_a-C_2\Gamma_t)\,,$$
$$\frac{d}{dx}a=-C_1(\Gamma_a a-tb)\,,\quad \frac{d}{dx}t=C_2(\Gamma_t t-ab)\,. \tag{40}$$

If we consider a strong pump which (slowly) increases in amplitude and look for solutions of the form $a,t\sim e^{\alpha x}$, where $\alpha\approx$ constant, we find

$$\alpha=\tfrac{1}{2}(C_2\Gamma_t-C_1\Gamma_a)\pm[\tfrac{1}{4}(C_2\Gamma_t+C_1\Gamma_a)^2-C_1C_2b^2]^{1/2}\,.$$

Modes A and T therefore have linear, decaying solutions below some threshold for pump mode amplitude, above which they exhibit oscillating behavior at a frequency which is pump-amplitude dependent.

For the undamped case $(\Gamma_a=\Gamma_t)=0$ Eqs. (40) can be rewritten to resemble those obtained for the usual three-wave backscatter problem

$$\frac{d}{dx}b-\Gamma^2\int b\,dx=-at\,,\quad \frac{d}{dx}a=tb\,,\quad \frac{d}{dx}t=-ab\,. \tag{41}$$

These equations are identical to the three-wave problem except for the Γ^2 term in the beam equation. The effect of simple linear growth in the three-wave case would be represented by a term of the form $(-\Gamma b)$, rather than the form in Eq. (41) involving the integral.

In the absence of the Γ^2 term, Eqs. (41) have the well-known elliptic solutions

$$b=b(0)\mathrm{dn}\left[b(0)x,\frac{t(0)}{b(0)}\right]\,,\quad a=a(0)\mathrm{sn}\left[b(0)x,\frac{t(0)}{b(0)}\right]\,,$$
$$t=t(0)\mathrm{cn}\left[b(0)x,\frac{t(0)}{b(0)}\right]\,.$$

A numerical integration of the undamped four-wave equations for the case $\Gamma=0$ is shown in Fig. 6 to verify the accuracy of the program. Figure 6(a) shows one set of periodic solutions. As mentioned earlier, these solutions are not time asymptotically stable, and will evolve in time into the decaying hyperbolic functions shown in Fig. 6(b). These latter solutions represent the unique final state possible for the system and occur independent of the initial conditions imposed upon the system.

For nonzero Γ, the undamped four-wave equations can be solved as for the time case:

$$\frac{d^2}{dx^2}b+[2(c_1t^2-c_2a^2)-\Gamma^2]b=0\,,$$
$$a=a_0\sin\left[(c_1c_2)^{1/2}\int_0^x b\,dz'+\phi_0\right]\,,$$
$$t=(c_2/c_1)^{1/2}a_0\cos\left[(c_1c_2)^{1/2}\int_0^x b\,dz'+\phi_0\right]\,,$$

where

$$\phi_0=\tan^{-1}\left[\left(\frac{c_1}{c_2}\right)^{1/2}\frac{a(0)}{t(0)}\right]\,,\quad a_0=\frac{c_1}{c_2}t^2(0)+a^2(0)\,.$$

These equations show that in the absence of any dissipation in the plasma modes and for conditions relevant to the experiment, no turning point is possible in the equation for $b(x)$. Only growing or oscillatory solutions exist which depend upon the relative values of $a(0)$, $t(0)$, and Γ. This is shown in Fig. 7 which illustrates the two types of spatial profiles obtained for the undamped four-wave equations over a wide range of input conditions. For $b(0)$ below some threshold values, the interaction is simply a strong-pump coupling of modes A and T with no stabilizing effects on the beam-plasma mode evident. For $b(0)$ above the threshold value, all modes exhibit periodic bounded behavior, but no region of linear growth is evident in the beam-plasma mode which would properly model the experimentally observed spatial profile. In addition, the proper boundary condition on $T(x=\mathfrak{L})$ is not met for these conditions. Since the proper combination of linear behavior and boundary conditions is not satisfied, we conclude that the undamped equations cannot model the physical system.

The introduction of dissipation to the plasma modes has a dramatic effect on the mode profiles. Since $v_{gT}<0$, any decay of mode T in the linear region appears as growth along the beam direction and can introduce a turning point in the equation for mode B. There is no reason to expect *a priori*, however, that this dissipation will produce distinct linear and nonlinear regions, and simultaneously satisfy the boundary condition that $T(x=\mathfrak{L})$ be small.

Since $\Gamma_a\ll\Gamma_t\ll\Gamma$, we can describe the initial develop-

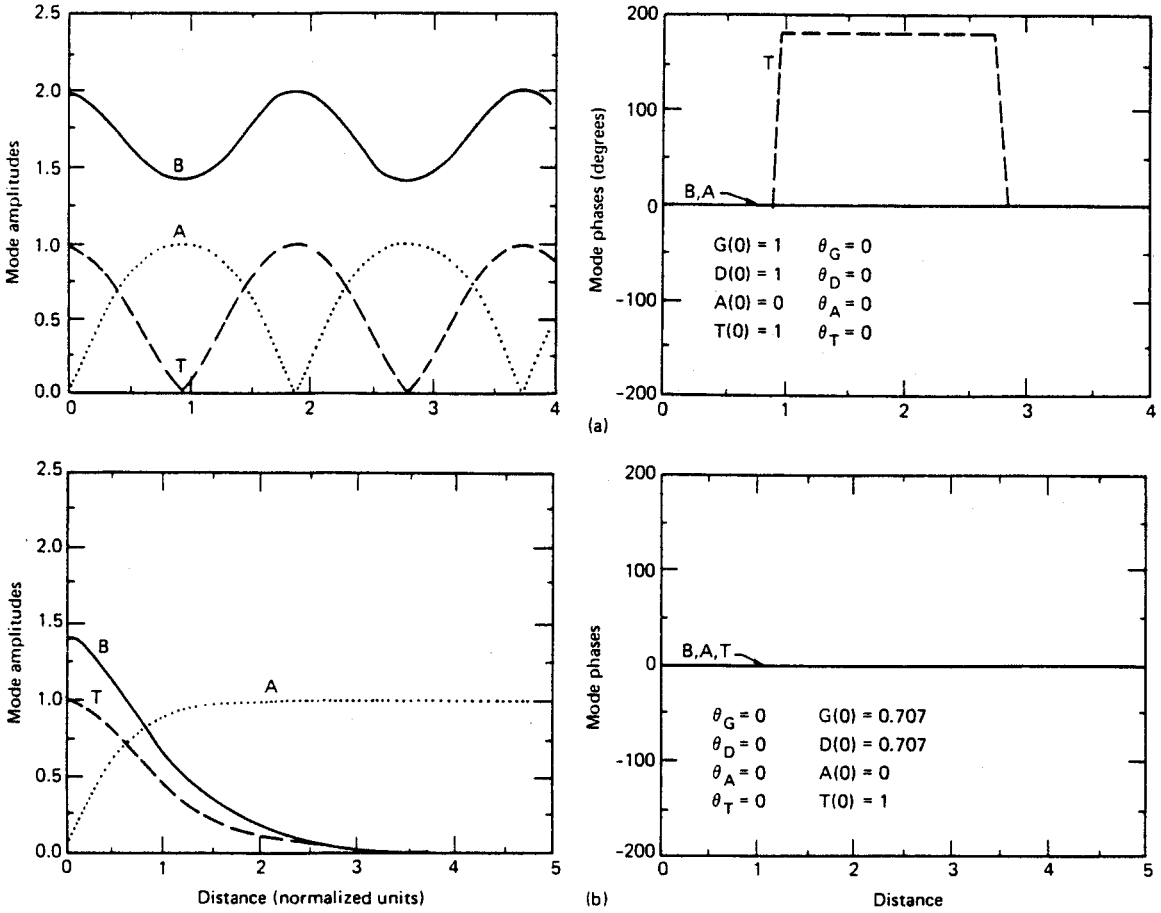

FIG. 6. Numerical solutions to the time-independent equations for the three-wave ($\Gamma = 0$) case, showing the (a) periodic and (b) fundamental solutions.

ment of the damped system by the equations

$$b = b_0 e^{\Gamma x}, \quad t = t_0 e^{\Gamma x}, \quad (d/dx)a = c_1 t b . \tag{42}$$

A turning point for this system can be shown to exist for $t(0)$ greater than some threshold value and is given by

$$x_t \approx \frac{1}{2\Gamma} \ln\left(\frac{\Gamma_t}{\Gamma}\xi\right),$$

where ξ is a normalizing factor such that $a(0) = 1$. Numerical integration of the four-wave equations with dissipation reveals that solutions exist for $|\theta_k| < 45°$ which exhibit distinct linear and nonlinear regions, satisfy the the condition that $T(x = \mathcal{L})$ be small, and show stabilizing effects due to pump depletion. An example of the spatial distribution obtained for boundary conditions and damping rates relevant to the mode coupling experiment is shown in Fig. 8. The solution is valid only over the range $0 < x < \mathcal{L}$, and in this range the turning point in $b(x)$ predicted by Eq. (42) clearly exists. Although in this example $b(x)$ renews its growth near the end of the system, concurrent with rapid oscillations of the plasma modes, the exact mode behavior in this region is extremely sensitive to the value of $t(0)$ used in the integration. Somewhat smaller values of $t(0)$ exhibit oscillating solutions for $t(x)$ without a turning point in $b(x)$, while larger values of $t(0)$ exhibit oscillations in $b(x)$ without $t(x = \mathcal{L})$ being small. Solutions could not be found which exhibit spatially decaying nonlinear behavior for all modes; however, the demands of computer time did not permit a wide range of conditions to be studied. These fundamental solutions may exist for only specific boundary conditions or in the time-asymptotic sense, as for the analogous three-wave backscatter case. Such an analysis is beyond the present scope of this work.

Using the numerically derived turning point distance (x_T) and mode amplitude $B(x_T)$ as a measure of saturation level we can perform sensitivity studies involving the dependence of x_T and $B(x_T)$ upon equation parameters, as was done for the time case. The results for the spatial system similarly show that both $B(x_T)$ and Γx_T are insensitive to the values of $B(x = 0)$ and scale with Γ approximately as $x_T \sim \Gamma^{-1}$ and $B(x_T) \sim \Gamma$. More importantly, the turning point amplitude also exhibits the strong dependence on θ_k which is observed for the time case, as shown in Fig. 9. The error bars reflect the large number of integrations required for each value of θ_k to find the range of $t(0)$ values involving the most strongly saturated beam-plasma mode. For $|\theta_k| < 45°$, parametric decay is always found to have a stabilizing influence on the growth of the unstable beam-plasma wave. Although the nonlinear interaction is not explosively unstable for $|\theta_k| > 45°$, in this regime the unstable growth of the beam-plasma mode continues unperturbed over the nonlinear region, while modes A and T periodically exchanges energy at a rate proportional to the amplitude of the growing mode.

IV. SCALING RELATIONS APPLIED TO EXPERIMENTS

Varational studies of the time and space-independent coupled mode equations have indicated that the saturation amplitude of the unstable beam-plasma wave depends most strongly upon the parameters Γ and θ_k, and therefore scales approximately as

$$E_S = \frac{\alpha_1(\exp \alpha_2\theta_k)}{|K|}, \tag{43}$$

where α_1 and α_2 are proportional constants. Although it has been noted that $|K|$ has a strong resonance near $v_B = v_b$, the most sensitive dependence of E_S is clearly upon the phase angle of the coupling coefficient. The value of these quantities can be evaluated from the linear dispersion characteristics of the modes, and their variation studied when system parameters such as beam energy, operating frequency, and so on are changed. In this section we compare such behavior with that observed in several beam-plasma experiments.

The dispersion relation describing the general beam-plasma instability is given by

$$\mathcal{K}_p(\omega, \mathbf{k}) = \eta[\omega_{pe}^2/(\omega - \mathbf{k}\cdot\mathbf{v}_b)^2], \tag{44}$$

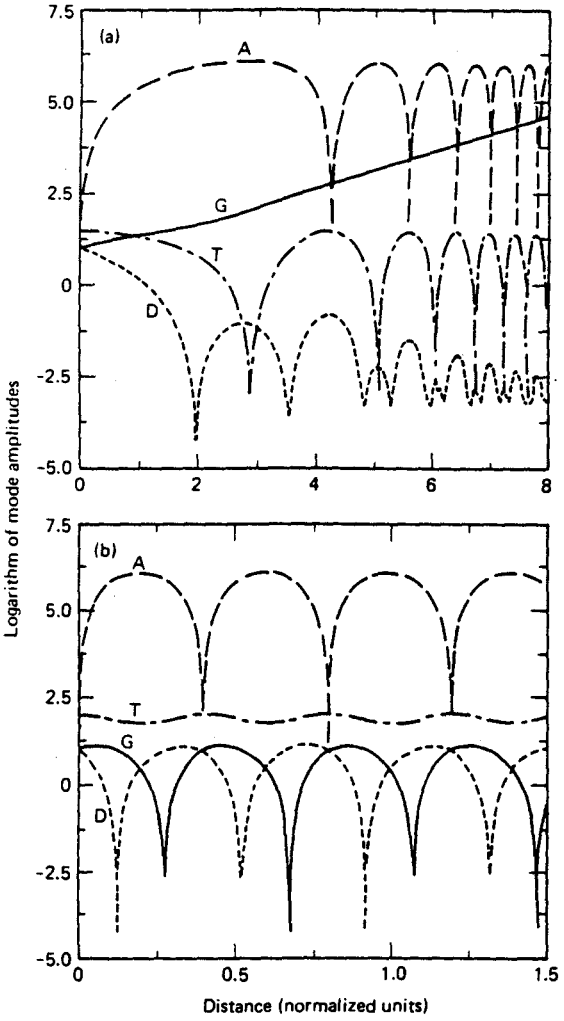

FIG. 7. Numerical integration of time-independent equations for modes D, G, A, and T, with $\Gamma_A = \Gamma_T = 0$, showing cases for $T(0)$ below (a) and above (b) threshold for stabilization of growing beam-plasma mode.

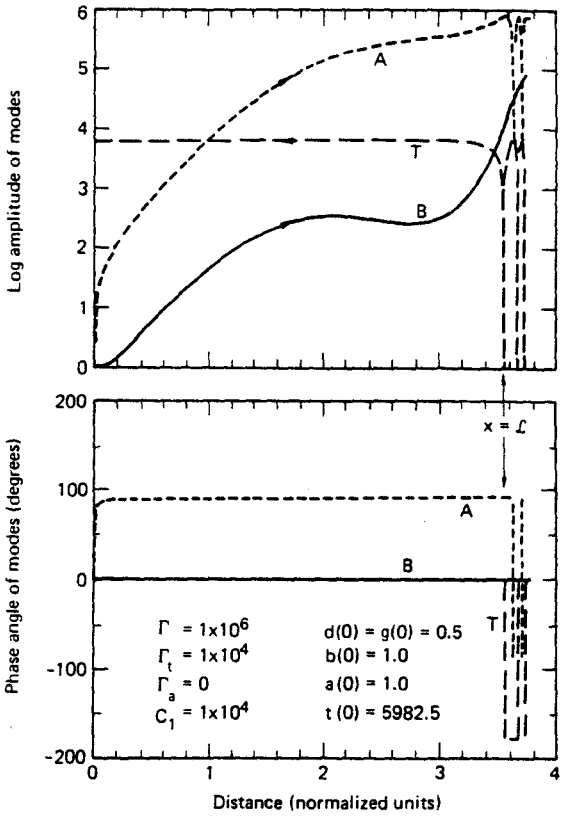

FIG. 8. Spatial evolution of modes B, A, and T with nonzero Γ_A and Γ_T, evaluated for experimental parameters, and showing stabilizing effects of parameteric decay. Solution is only valid between $0 < x < £$.

where $\mathcal{K}_p(\omega, \mathbf{k})$ is the relative dielectric constant for the background plasma. The simplest expression for the reactive high-frequency instability can be obtained from Eq. (8) by ignoring thermal and ion effects

$$\frac{k^2}{k_z^2} = \frac{\omega_{pe}^2}{\omega^2}\left(1 + \eta\frac{\omega^2}{(\omega - k_z v_b)^2}\right). \tag{45}$$

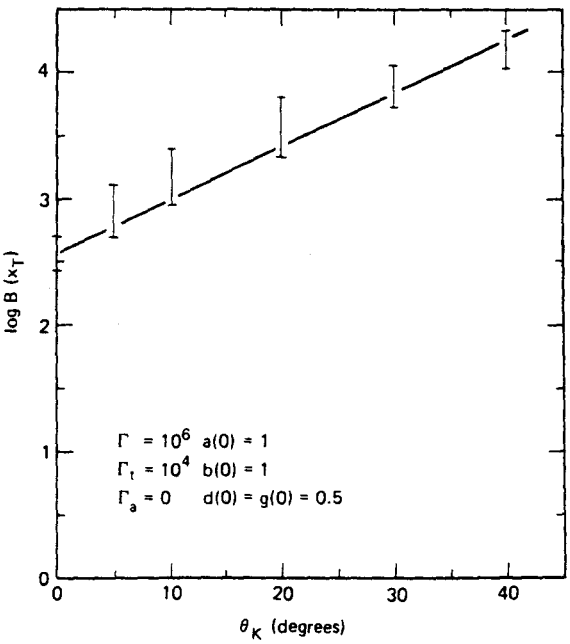

FIG. 9. Dependence of turning point amplitude upon phase angle of the coupling coefficient.

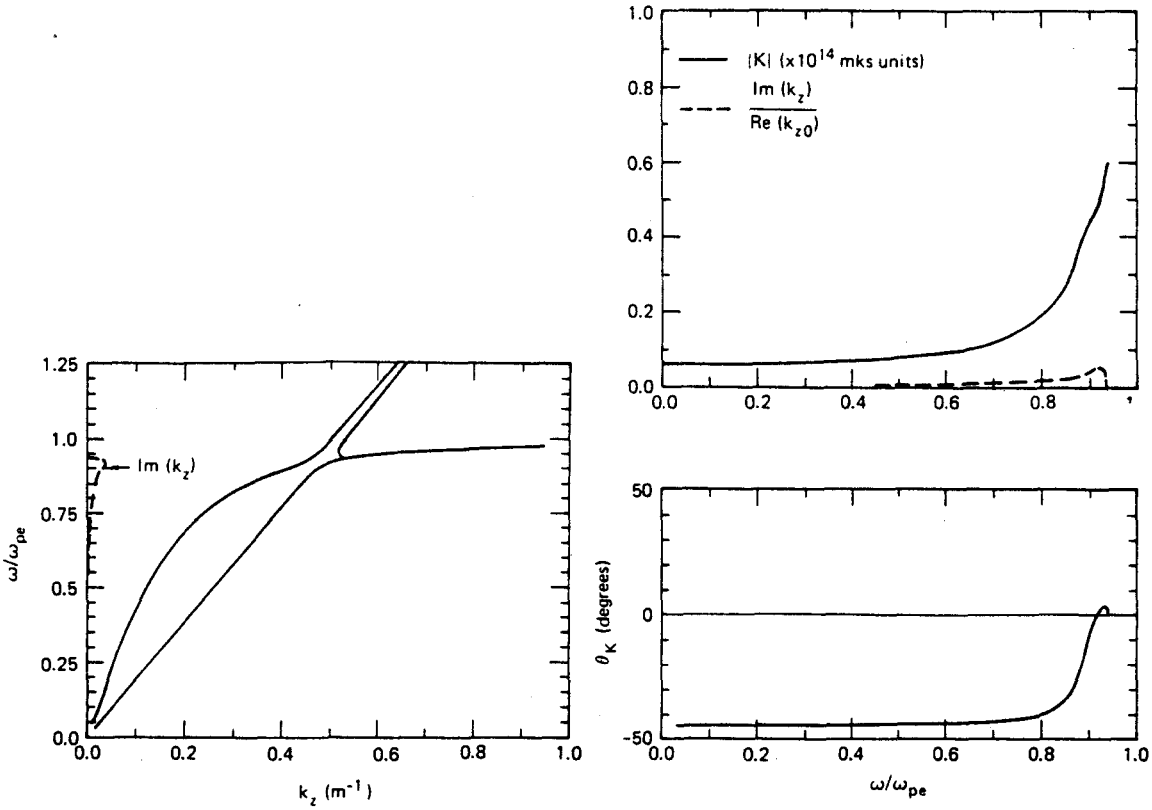

FIG. 10. The dispersion relation and coupling coefficient evaluated for the wave-coupling experiment: $n_0 = 3\times10^{10}$ cm^{-3}, $U_b = 1000$ V, $I_b = 1$ mA, $k_\perp = 210$ m^{-1}.

In Eq. (29) we saw that the complex nature of $\tilde{K}$ is essentially determined by the factor $\tilde{U}_B^{1/2}$, which is given in its simplest form corresponding to Eq. (45) by

$$\tilde{U}_B = 1 + \eta(1 - v_b/\tilde{v}_B)^{-3}. \tag{46}$$

For the case of spatial growth, we assume a fixed (real) frequency and look for complex wavenumber $\tilde{k}_z = \omega/v_b + \tilde{\Delta}$. For low-frequency modes $\omega \ll \omega_0$, where (ω_0, k_0) denotes the mode corresponding to maximum growth, we can ignore corrections to $\mathcal{K}_b$ in Eq. (44) and find

$$\tilde{\Delta} = \eta \frac{\omega_{pe}^2}{v_b^2} \frac{\omega^2}{k_\perp^2 v_b^2 - \omega_{pe}^2}.$$

In this region we have spatial growth for dense plasmas where $\omega_{pe} > k_\perp v_b$, which is the case for the wave-coupling experiment considered here. In this limit $\tilde{U}_b = j\eta^{-1/2}$, so that $\theta_k = -45°$, and one expects relatively large saturation amplitudes. For the less dense case, $\tilde{\Delta}$ has real solutions, and the phase angle of the coupling coefficient should be correspondingly small. For operating frequencies near ω_0, we are forced to include corrections to $\mathcal{K}_b$, as can be seen from the dispersion characteristics in Fig. 1. Keeping only first-order corrections to k_z we find

$$\left(1 - \frac{v_b}{\tilde{v}_B}\right)^3 = -\tilde{\Delta}^3\left(\frac{v_b}{\omega}\right)^3 = -\frac{\eta}{2}\left(\frac{\omega_{pe}}{k_\perp v_b}\right)^2.$$

Since $\tilde{U}_B^{1/2}$ involves the cubic quantity directly, $\tilde{\Delta}$ is purely real and θ_k should vanish near the region of maximum growth. The saturated field strength due to wave coupling should therefore be smallest in this region, and it is significant that the strongest decay spectra are observed experimentally by tuning to this region. For higher frequency modes $\omega > \omega_0$, the wavenumber shift again becomes complex so that θ_k is nonzero. As the operating frequency approaches cutoff and the growth rate vanishes, $\tilde{U}_B$ again becomes real and θ_k should vanish.

This variation in θ_k, and the correspondingly large range in saturated wave amplitudes, can cause transitional behavior in saturation mechanisms. This behavior is more evident in Fig. 10, which shows the dispersion relation numerically evaluated for the wave-coupling experiment, along with the corresponding variation of the magnitude and phase of the coupling coefficient with operating frequency. The exact roots corresponding to the beam-plasma mode are evaluated using Eq. (8), and Eq. (29) is then used to evaluate the coupling coefficient. The frequency dependence and absolute value of $|K|$ and θ_k agree with that predicted in the limits discussed. It is clear that very near (ω_0, k_0), both the resonance in $|K|$ and the vanishing of θ_k contribute to minimize the saturated field strength. The behavior of $\tilde{K}$ at lower frequencies, however, indicates that the saturated field strength will increase significantly for $\omega < \omega_0$. This suggests that the growth of the beam-plasma modes near (ω_0, k_0) may be stabilized by pump depletion at a level below which other nonlinear mechanisms can occur, while other mechanisms could dominate the nonlinear development of the system for lower frequency modes. This frequency dependence of saturated field strength has been observed both in the wave coupling ex-

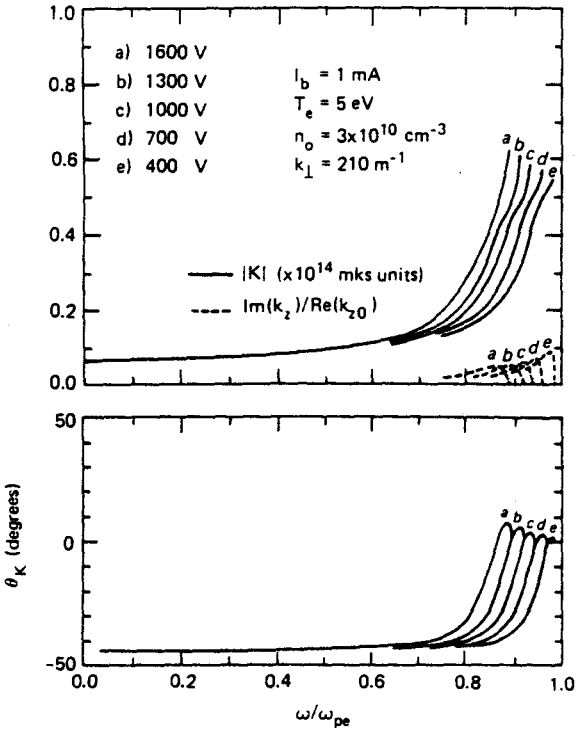

FIG. 11. Magnitude and phase of coupling coefficient versus frequency for several values of beam energy.

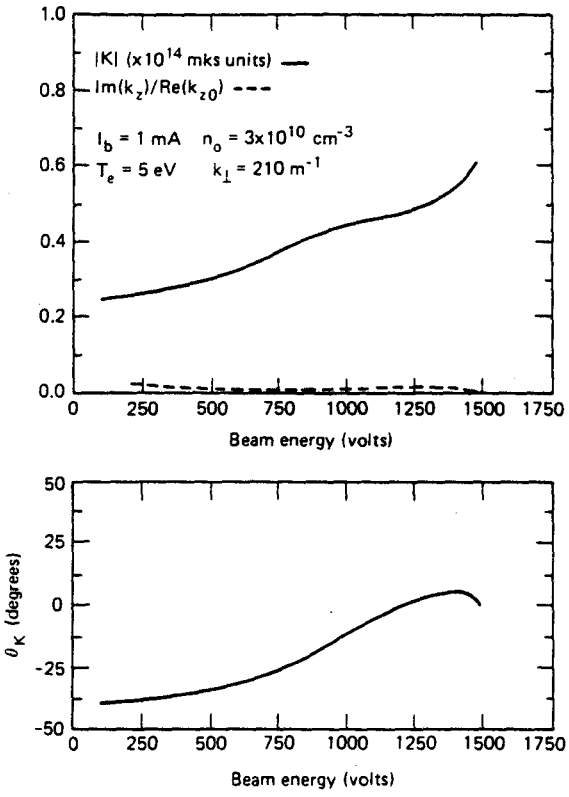

FIG. 13. Magnitude and phase of coupling coefficient versus beam energy for wave-coupling experiment. Values obtained for $\omega/\omega_{pe} = 0.9$.

periment and by Jones *et al.*,[4] where modes near (ω_0, k_0) saturated via parametric decay while lower-frequency modes saturated by beam trapping.

By numerically evaluating the dispersion relation and coupling coefficient for varying experimental conditions, one can study the regions over which the decay instability might dominate over other saturation mechanisms. Figures 11 and 12 show two such cases, where we plot the frequency dependence of $|K|$ and θ_k under conditions of experimental interest for several values of beam energy and background plasma density. The general frequency dependence of θ_k changes little over a broad range of beam energies, although for a fixed operating frequency the value of θ_k will remain sensitive to beam energy. This latter case is shown in Fig. 13, where we plot $|K|$ and θ_k as a function of beam energy over a range accessible to the experiment. It is clear that E_S should increase significantly at lower beam energies, and this is consistent with experimental observations that beam energies in excess of about 800 V are required to obtain strong decay sidebands.

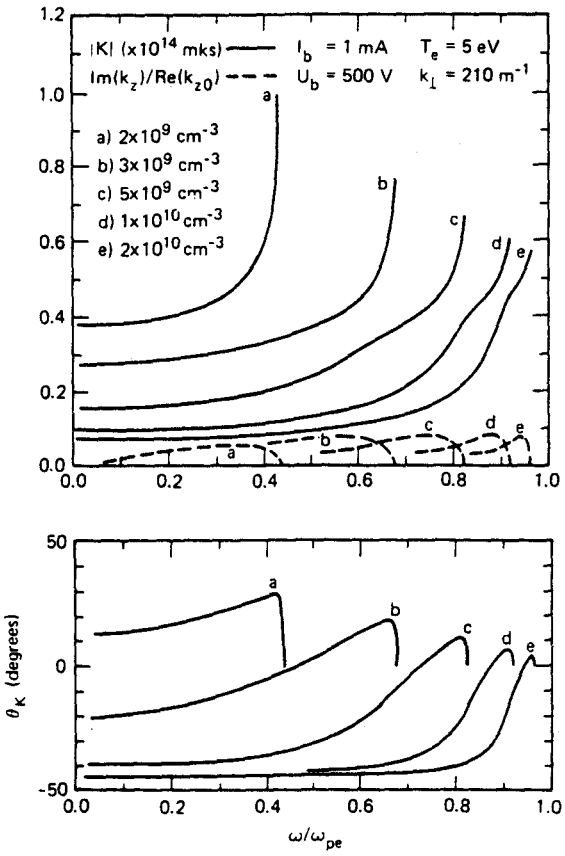

FIG. 12. Magnitude and phase of coupling coefficient versus frequency for several values of background plasma density.

The frequency profile of θ_k changes significantly as one reduces the background plasma density, as shown in Fig. 12. For experiments involving low frequency modes and lower density plasmas, θ_k is reduced from its value at high densities as discussed previously. For modes operating near that of maximum growth, however, it can be seen that the coupling coefficient becomes complex as the background density is reduced, and the mode where θ_k vanishes shifts to lower frequencies. For low-density experiments, therefore, E_S should remain large over the most unstable portion of the frequency spectrum, and stabilization mechanisms other than pump depletion by parametric decay may be important. Similar studies concerning the variation of $|K|$ and θ_k with beam current and plasma radius indicate that E_S is insensitive

TABLE II. Parameters of several beam-trapping experiments.

Author	No(cm^{-3})	$U_b(v)$	ω_0/ω_{pe}
Gentle (Ref. 14)	1×10^9	300	0.50
Nyack (Ref. 15)	3×10^8	100	0.62
DeNeef (Ref. 15)	5×10^8	150	0.67
Malmberg (Ref. 15)	5×10^8	100	0.73

to beam current except at low values ($i_b \lesssim \frac{1}{2} mA$), where θ_k begins to deviate from small values. The variation of $|K|$ and θ_k with radial wavenumber is similar to that obtained for a variation in background density, with the frequency corresponding to $\theta_k = 0$ decreasing with larger wavenumber. Over the large range of system parameters studied, a case was never observed with $|\theta_k| > 45°$, suggesting that the decay process can never act as a destabilizing mechanism to the linear beam-plasma instability.

Beam trapping has been conclusively identified as the dominant saturation mechanism in several weak beam-plasma experiments,[14,15] however, most of these experiments share a common region of parameter space, as summarized in Table II. In general, they seem to have utilized a low density background plasma and beam parameters such that the ratio ω_0/ω_{pe} is much less than unity. Figure 14 shows the dispersion relation numerically evaluated for one such experiment, whose parameters are typical of that for all other trapping cases studied.[14] The numerical results predict a mode of maximum growth whose frequency is consistent with the ratio measured. The corresponding plots of $|K|$ and θ_k in Fig. 14 show that for these cases θ_k is large over the entire unstable frequency spectrum, suggesting that the saturated field strength due to parametric decay is substantially larger than that for the wave-coupling experiment described previously. At the same time, the relatively small values of $(v_b - v_B)$ for these cases predict that the field strength required to stabilize the unstable beam-plasma mode by beam trapping is small

$$E_T = 4k_B U_b (1 - v_B/v_b)^2 . \tag{47}$$

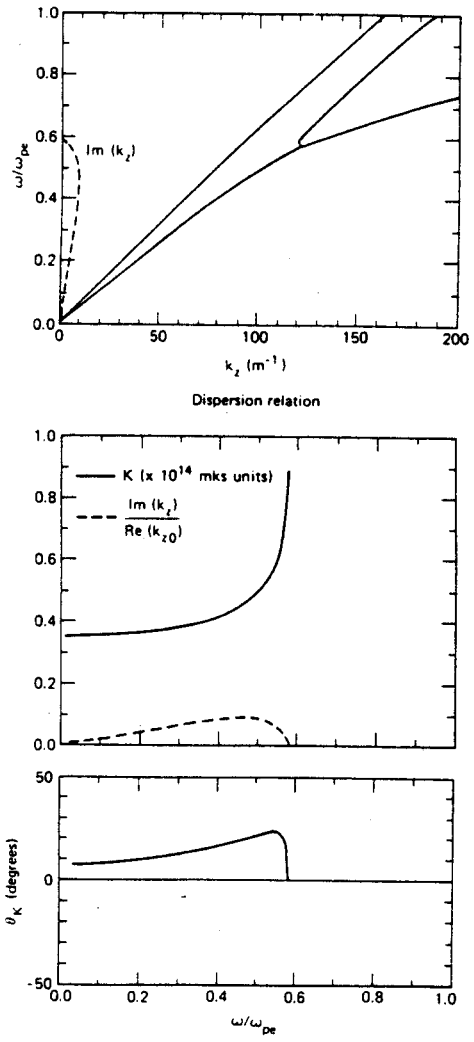

FIG. 14. The dispersion relation and coupling coefficient evaluated for a beam trapping experiment: $n_0 = 1\times10^9$ cm^{-3}, $U_b = 300$ V, $I_b = 1$ mA, $k_\perp = 190$ m^{-1}.

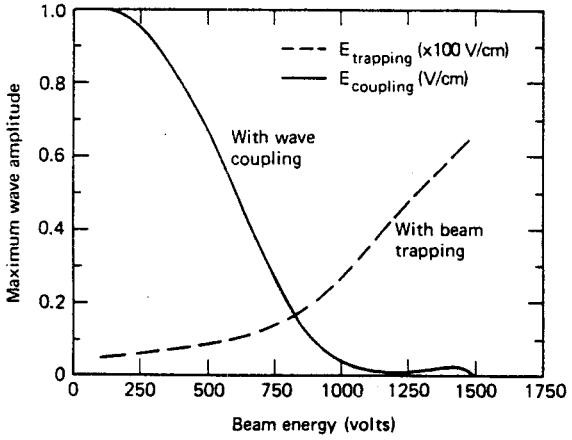

FIG. 15. Saturated field strength, due to wave coupling and beam trapping, versus beam energy. Assumed conditions: $n_0 = 3\times10^{10}$ cm^{-3}, $I_b = 1$ mA, $k_\perp = 210$ cm^{-1}, $\omega/\omega_{pe} = 0.9$.

Figure 15 compares the variation of saturated field strength with beam energy for both parametric decay and beam trapping under conditions relevant to the wave coupling experiment, using the numerical scaling of Sec. III and Eq. (47). While the absolute field strengths calculated are subject to the errors discussed earlier, it is evident that wave coupling and beam trapping effects may act as competing saturation mechanisms, with each dominating over a different parameter range.

An example of such a transition in nonlinear behavior is presented in Fig. 16, which shows three photographs of the high-frequency spectra of the decay instability described previously in Fig. 2. For $U_b = 1100$ V a well-defined decay sideband spectrum of TG modes is seen below the entrained beam-plasma wave. Except for the corresponding spectrum of IA modes, no other spectra are present along the length of the system. At 900 V the decay spectrum is weakened and paired sidebands begin to appear at a lower difference-frequency from the main wave. At lower beam energies the narrow, low-frequency sidebands largely dominate the spectrum. The decay spectrum is insensitive to beam current, while the frequency of the low-frequency sidebands vary

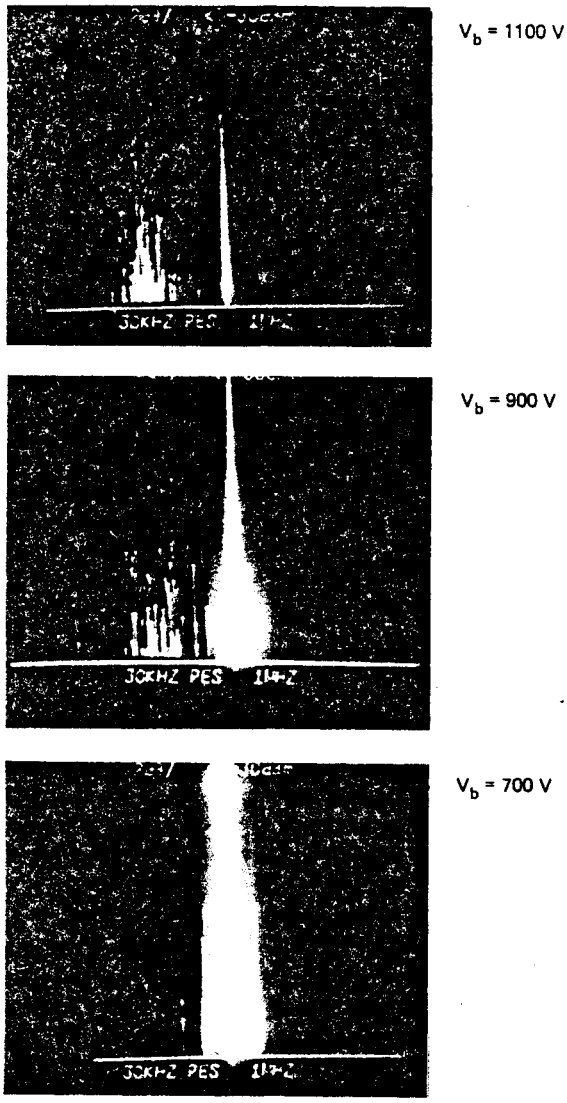

FIG. 16. High frequency spectrum of the beam plasma instability for several values of beam energy.

strongly with beam current. Although the origin of the low-frequency sidebands has not been investigated, their sharp resonant nature and strong frequency- and amplitude-dependence upon the beam-plasma wave amplitude suggest that they may be linear sidebands which arise as precursor to trapping sidebands,[16] and suggest the onset of another saturation mechanism.

V. CONCLUSION

A formalism has been derived to study the nonlinear evolution of the reactive beam-plasma instability due to wave-coupling. The results require a four-wave model for the interaction and indicate that pump depletion can stabilize the growth of the linear instability at levels below which other nonlinear mechanism become important. Sensitivity studies show that this can occur over a side range of experimental conditions. The range of plasma density, beam energy, and mode frequencies over which strong parametric coupling has been observed is consistent with this model. The model also predicts transitional behavior between parametric and beam-trapping effects which has been observed in two experiments. This arises due to a variation in the phase angle (or real part) of the beam-plasma mode energy. This variation causes a corresponding change in the maximum field amplitude due to parametric decay and an inverse dependence in field amplitude due to beam trapping. The range of experimental conditions over which beam trapping has been observed seem consistent with this model. For the range of parameters studied to date, parametric effects dominate at the mode of maximum linear growth and for the stronger beam-plasma instabilities where $(1 - v_B/v_b)$ is not small. The issues involving the time-asymptotic spatial mode profiles need to be resolved and should provide further insight into the long-term evolution of the beam-plasma instability and wave-coupling mechanisms in general.

ACKNOWLEDGMENTS

The authors would like to acknowledge useful discussions with Dr. M. Tekula and Professor K. Bender.

This work was supported by the National Science Foundation under Grant No. GK-28282X1 and by the U.S. Department of Energy, Contract No. ET-78-C-01-3019.

[1]M. Seidl, Phys. Fluids **13**, 966 (1970); J. Apel, *ibid.* **12**, 291 (1969); R. Briggs, *Electron-Stream Interactions with Plasmas* (MIT Press, Cambridge, Mass., 1964).
[2]M. Seidl, W. Carr, D. Boyd, and R. Jones, Phys. Fluids **19**, 78 (1976); H. Ikezi, R. Chang, and R. Stern, Phys. Rev. Lett. **36**, 1047 (1976).
[3]R. Parker and A. Throop, Phys. Rev. Lett. **31**, 1549 (1973).
[4]R. Jones, W. Carr, and M. Seidl, Phys. Fluids **19**, 607 (1976).
[5]A. Throop, Ph.D. thesis, Massachusetts Institute of Technology (1976).
[6]B. Quon, A. Wong, and B. Ripin, Phys. Rev. Lett. **32**, 406 (1974); C. Nyack and P. Christiansen, Plasma Phys. **17**, 249 (1974); J. A. Ca. Cabral, Plasma Phys. (N.Y.) **18**, 719 (1976).
[7]B. Coppi, M. N. Rosenbluth, and R. Sudan, Ann. Phys. **55**, 207 (1969).
[8]A. Bers and P. Penfield, IRE Trans. Electron Devices **ED-9**, 12 (1962).
[9]W. Allis, S. Buchsbaum, and A. Bers, *Waves in Anistropic Plasmas* (MIT Press, Cambridge, Mass., 1963).
[10]G. Schmidt, Phys. Fluids **18**, 1218 (1975).
[11]R. Harvey and G. Schmidt, Phys. Fluids **18**, 1395 (1975).
[12]V. Fuchs and G. Beaudry, J. Math. Phys. **17**, 208 (1976).
[13]N. Rostoker, Nucl. Fusion **1**, 101 (1961).
[14]K. Gentle and J. Lohr, Phys. Fluids **16**, 1464 (1974).
[15]C. Nyack and P. Christiansen, Phys. Fluids **17**, 2025 (1974); C. DeNeef, J. Malmberg, and T. O'Neil, Phys. Rev. Lett. **30**, 1032 (1973); J. Malmberg and C. Wharton, Phys. Fluids **12**, 2600 (1969).
[16]G. Morales and J. Malmberg, Phys. Fluids **17**, 609 (1974).